

Daniela Teodor (1), Laura Pinzon-Rincon (1), Aurélien Mordret (1,2), François Lavoué (1,2),
Sophie Beaupretre (2), Charles Beard (1,2), Pierre Boué (1), Florent Brenquier (1)

PRESENTED AT: AGU 2020



**High-frequency passive surface wave tomography at the Marathon PGE-Cu deposit (Ontario, Canada):
Bridging the gap between natural and anthropogenic noise sources**

Daniela Teodor (1), Laura Pinero-Rincon (1), Amelia Morfin (1,2), François Lavoie (1,2), Sophie Desjardins (2), Charles Beaud (1,2), Pierre Boad (1), Flavien Drogachev (1)

(1) Université de Guelph, (2) Géosciences Québec

1. Context and data set

Background:

- This study aims at imaging with relatively high-resolution the "shallow" ($< 2 \text{ km}$ -depth) velocity structure of the Marathon Cu-PGE system through ambient noise surface-wave tomography while mitigating the signals generated by natural and anthropogenic noise sources.

2. Sources of noise

Broadbanding analysis of the recorded data indicates variations in the distribution of noise [Figure 2]

3. Surface wave tomography

Marathon dense array

Data processing:

- The signal was filtered sampled from 200 Hz to 10 Hz, divided into segments of 30 minutes, cross-correlated and time stacked.

Phase velocity analysis and inversion

Marathon sparse array

- A secondary study was conducted where the Marathon sparse array is analysed for phase-velocity variations associated to different seismic events.

4. Phase velocity variation with the noise azimuth

5. References

Cole, F., J. Fournier, A. Desjardins, S. Bédard, C. Beaud, C. Lévesque, C. L. Bonin, A. Desjardins, R. Desjardins, C. O'Brien (2017). Shallow crustal stress fields under conditions of tectonic compression inferred from geophysical observations. *J. Geophys. Res.*, 122, 10, 10, 10, 10.

Desjardins, S. and O'Brien (2017). Rayleigh waves: An overview of their properties and applications. In: *Rayleigh Waves: Theory and Applications*. Springer, Cham.

The authors acknowledge funding provided by the research group of the University of Guelph (S.A. Desjardins, C. Beaud, et al.).

Funding:
GRC 580-17-0001 - Funding received from the Geological Survey of Canada (GSC).

1. CONTEXT AND DATA SET

Framework

- This study aims at imaging with relatively high-resolution the "shallow" (down to 1 km depth) velocity structure of the Marathon Cu-PGE deposit, through ambient noise surface wave tomography, while merging the signals generated by natural and anthropogenic noise sources.
- The Marathon deposit is one of the pilot tests of the passive seismic reflection technique in the H2020 PACIFIC project.

<https://www.pacific-h2020.eu/>

Geological context and data set

- The area of interest is located at 10 km N of the town of Marathon (Ontario-Canada) along the N shore of Lake Superior. Marathon is a disseminated Cu-PGE deposit hosted within the Eastern Gabbro of the Coldwell Complex, which is part of the Midcontinent Rift system. The gabbroic intrusion is surrounded by syenites and Archean metavolcanic breccia (*Figure 1* and *Video 1*).
- An aim of the Marathon experiment is imaging the footwall contact of the Coldwell Complex, and other structures that control the location of the mineralisation.
- 1024 vertical-component receivers were deployed for 30 days according to 2 overlapping grids (e.g. *Dales et al., 2020*):
 - a dense array (200 m x 6040 m), with a grid spacing of 50 m and
 - a sparse array (2500 m x 4000 m) with a grid spacing of 150 m.

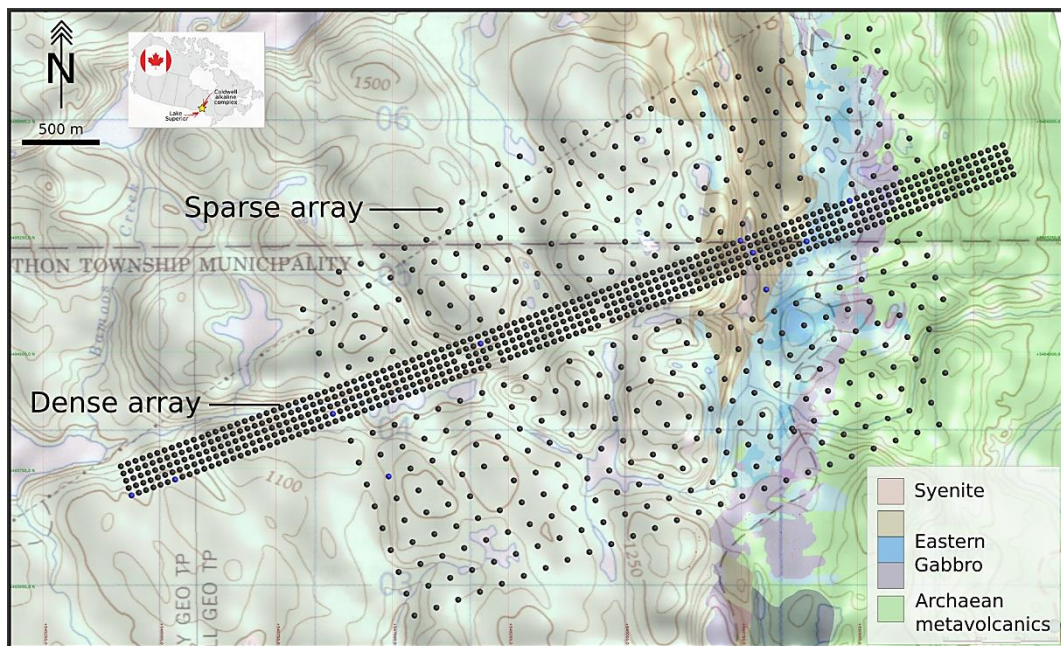


Figure 1 - Passive seismic acquisition design.

[VIDEO]

<https://www.youtube.com/embed/cE6pFuk3Rms?rel=0&fs=1&modestbranding=1&rel=0&showinfo=0>

Video 1 - The Marathon experiment.

2. SOURCES OF NOISE

Beamforming analysis of the recorded data indicates variations in the distribution of noise (Figure 2).

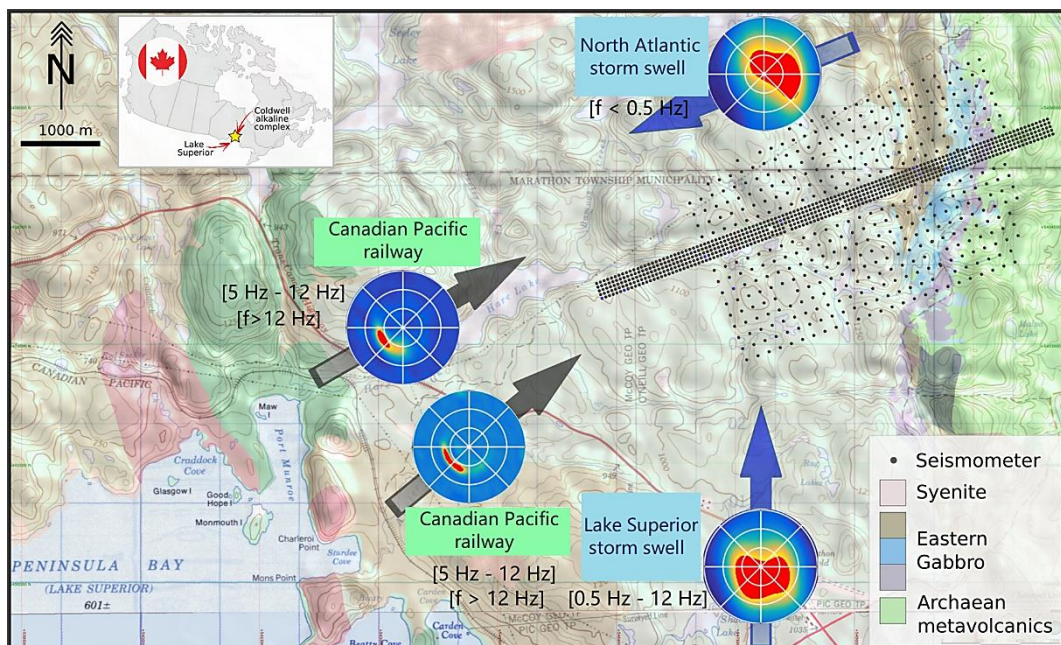


Figure 2 - The main sources of noise in the Marathon area.

Below 5 Hz, the noise has a natural origin, while above 12 Hz, the noise is anthropogenic. Different sources, acting from preferential azimuths, contribute to the Green's function construction:

- below 0.5 Hz: surface wave energy - waves in the Hudson Bay (NE);
- 0.5 - 5 Hz: surface wave energy - waves in the Lake Superior (SSW);
- 5 Hz - 12 Hz: surface wave energy: waves in the Lake Superior (SSW), trains from Canadian Pacific Railway (SW) and vehicles from Trans Canada Highway (SW);
- 12 Hz - 20 Hz: body wave energy combined with less energetic surface waves: trains and vehicles (SW);
- above 20 Hz: body wave energy: trains and vehicles (SW).

3. SURFACE WAVE TOMOGRAPHY

Marathon dense array

Data processing

- The signal was down-sampled from 250 Hz to 50 Hz, divided into segments of 30 minutes, cross-correlated and then stacked.

Phase velocity analysis and inversion

- As vertical-component sensors were deployed, the phase velocity corresponds to the Rayleigh wave velocity. In this study, only the fundamental mode of surface wave propagation was considered for the frequency - wavenumber (F-K) analysis.
- Surface wave dispersion curves were extracted using receiver arrays divided into segments of variable space extension (2 km, 1 km and 500m, respectively - Figure 3a, 5a and 6a). The shallow structures were reconstructed with progressively increased resolution, down to 1 km depth, 500 m depth and 250 m depth, respectively.
- Surface wave dispersion curves were retrieved from different virtual shot gathers. For each segment, an average dispersion curve was computed from dispersion curves belonging to 5 seismic lines.
- Each average dispersion curve was inverted to an S-wave velocity profile using an MCMC transdimensional Bayesian approach (Dreiling and Tilmann, 2019). The various S-wave velocity profiles were laterally merged and interpolated, leading to 2D S-wave velocity models.

a) 2 km long arrays

- 3 average surface wave dispersion curves were extracted from 2 km long arrays and inverted to S-wave velocity structures (Figure 3 and Figure 4). A frequency range of 1.5 Hz - 21 Hz was considered for the inversion.

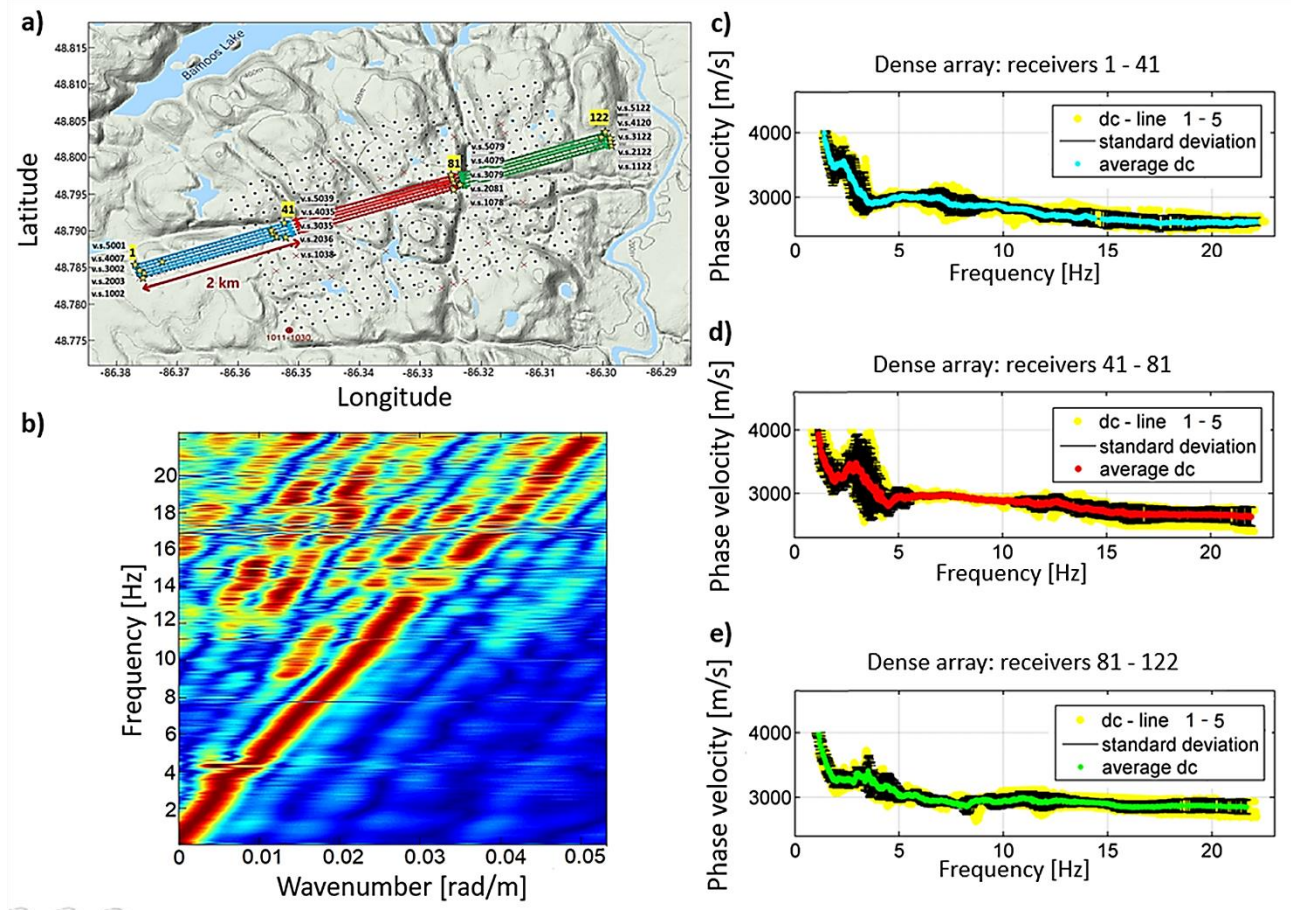


Figure 3 - Experiment design for the characterization of the subsurface structure down to 1 km depth. a) Array configuration for dispersion curves extraction. b) Example of F-K spectrum. c) Dispersion curves retrieved for the first segment of the dense array. d) Dispersion curves retrieved for the second segment of the dense array. e) Dispersion curves retrieved from the third segment of the dense array.

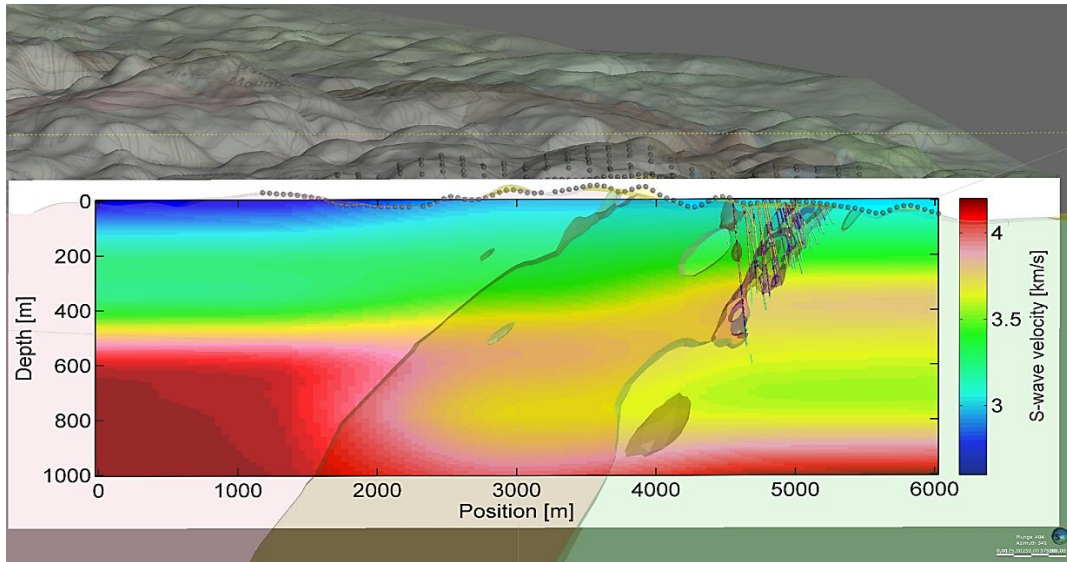


Figure 4 - S-wave velocity model obtained by merging and interpolating the vertical profiles.

b) 1 km long arrays

- 6 average dispersion curves were extracted from 1 km long arrays and inverted to S-wave velocity structures (Figure 5). A frequency range of 3 Hz - 21 Hz was considered for the inversion.

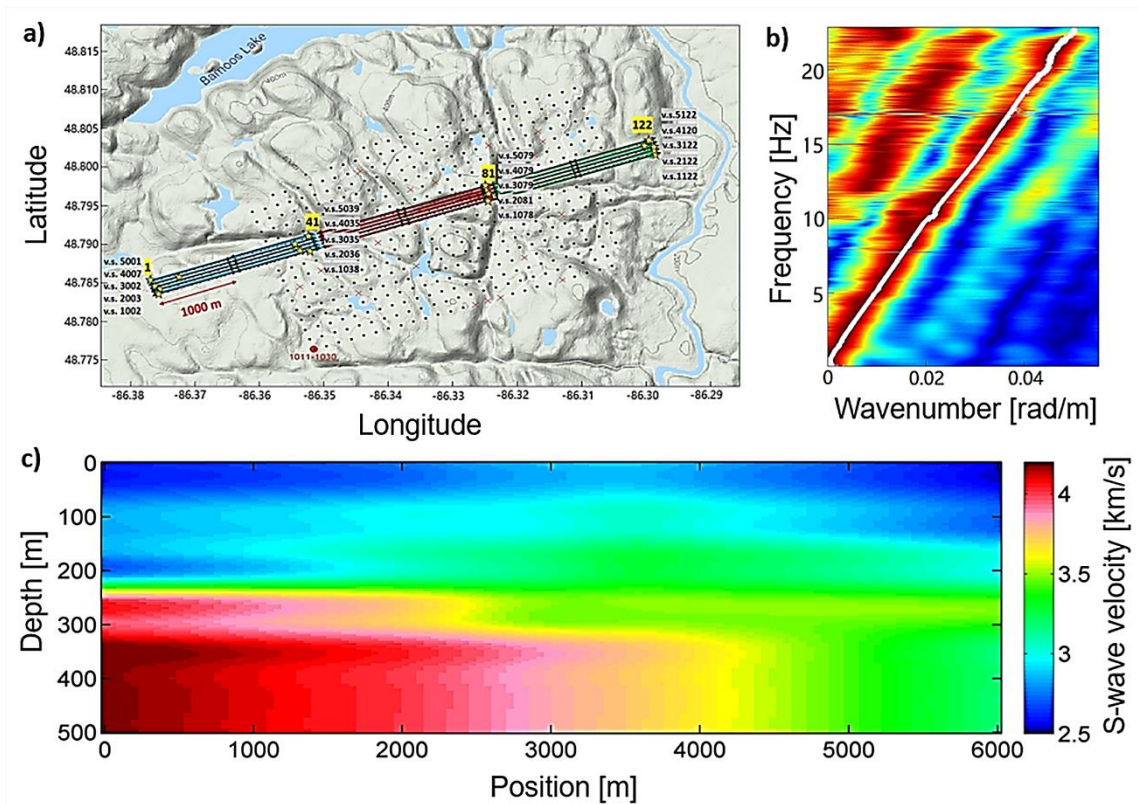


Figure 5 - a) Experiment design for the characterization of the subsurface structure down to 500 m depth. b) Example of F-K spectrum. c) S-wave velocity model obtained by merging and interpolating the vertical profiles.

c) 0.5 km long arrays

- 12 average surface wave dispersion curves were extracted from 0.5 km long arrays and inverted to S-wave velocity structures (Figure 6). A frequency range of 6 Hz - 21 Hz was considered for the inversion.

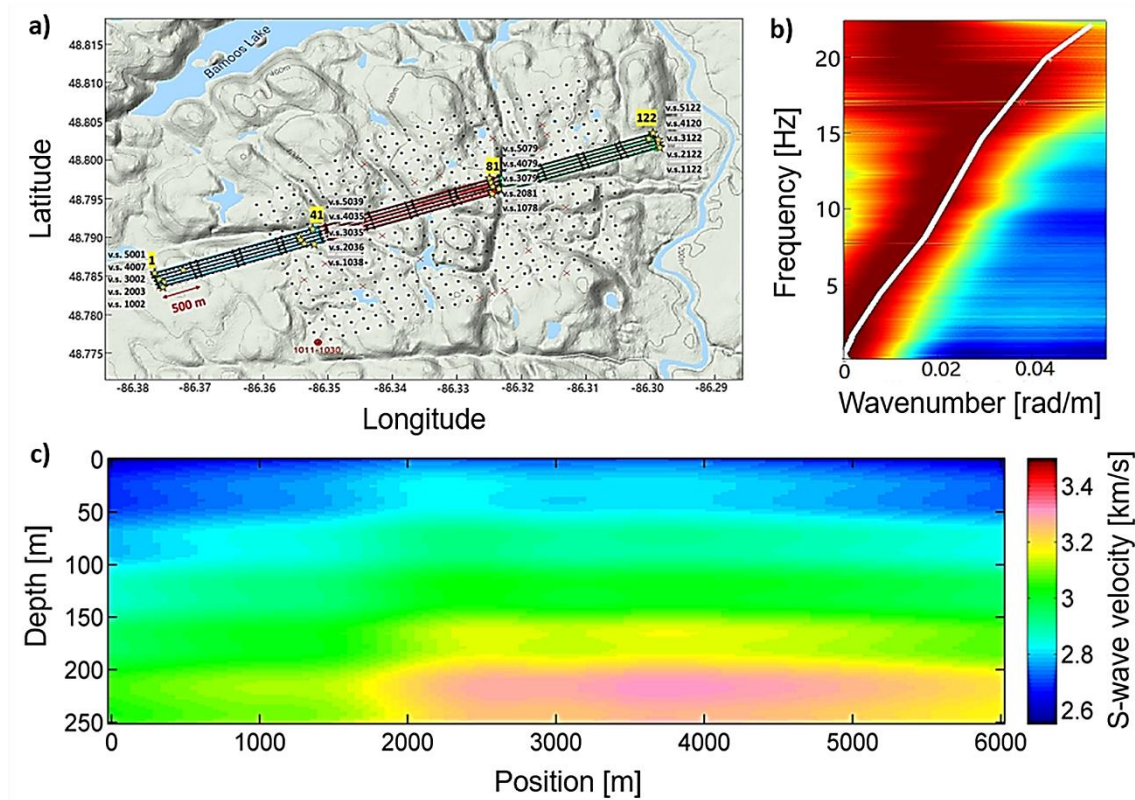


Figure 6 - a) Experiment related to the characterization of the subsurface structure down to 250 m depth. b) Example of F-K spectrum. c) S-wave velocity model obtained by interpolating the vertical profiles.

Take-home messages

- The large-wavelength structures in the S-wave velocity model are relatively consistent with the geological structures inferred from surface mapping and drill core data. Nevertheless, the sub-horizontal contacts noticed in the tomographic images do not reproduce faithfully the dipping angle of some geological structures (constrained by drill hole data, down to 600 m depth).
- A high-velocity anomaly, noticed in the dispersion curves and in the tomographic images at about 500 m depth, may be related to the mafic intrusion associated with the Cu-PGE mineralization.

4. PHASE VELOCITY VARIATION WITH THE NOISE AZIMUTH

Marathon sparse array

- A sensitivity study was conducted over the Marathon sparse array to analyze the phase velocity variation trend for different azimuths.

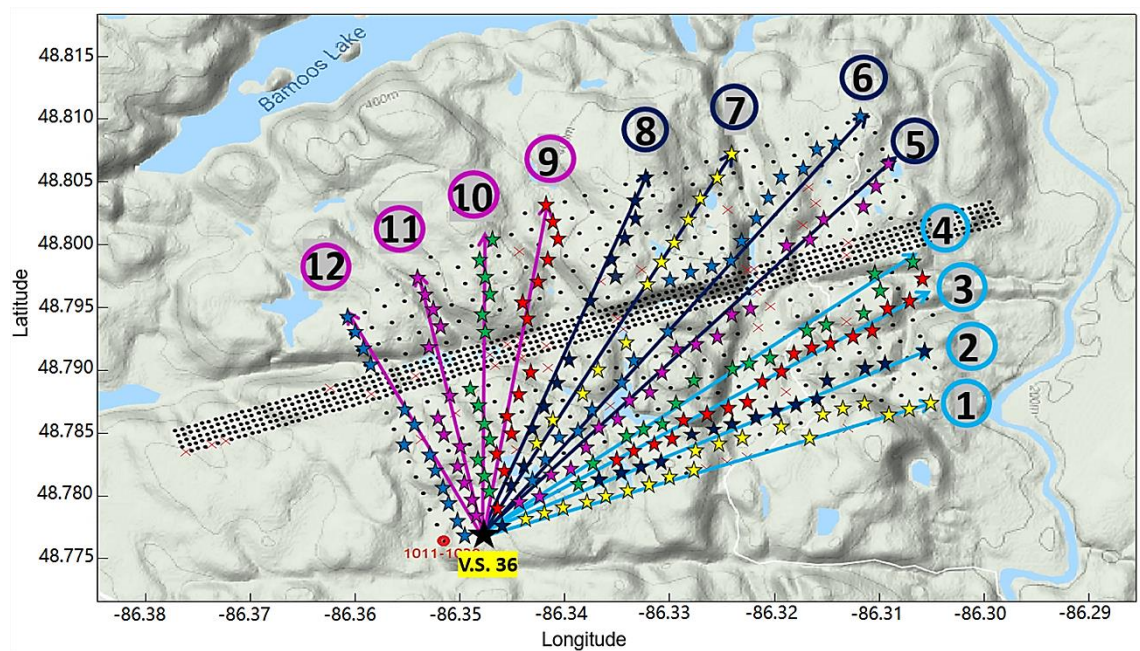


Figure 7. Marathon sparse array: sensitivity study of the phase velocity variation with the azimuth. The numbers from 1 to 12 indicate the different directions considered for the extraction of surface wave dispersion curves.

- Surface wave dispersion curves were extracted from receiver arrays distributed according to 12 different azimuths (indicated with numbers from 1 to 12 in Figure 7), using the same virtual shot (v.s. 36).
-
- A phase velocity variation, related to the change in noise characteristics and geological asset, is noticed for different azimuths (Figure 8).

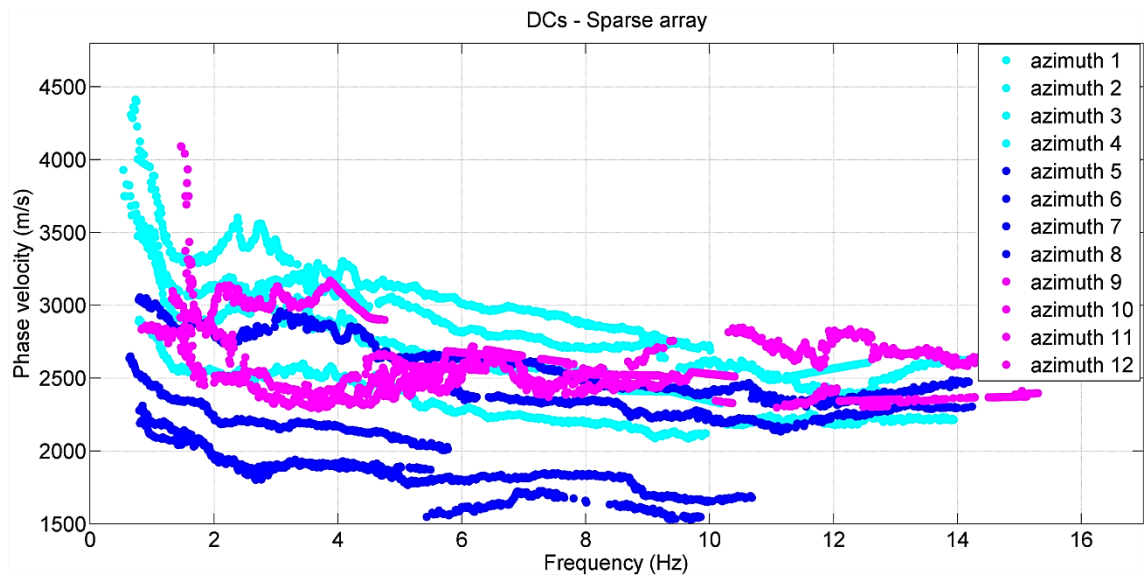


Figure 8. Dispersion curves extracted along the azimuths 1 to 12.

Future work

- Future work aims at retrieving a high-resolution S-wave velocity model for the shallow part of the entire investigated area, using the Marathon sparse array data. The final S-wave velocity model will be reconstructed from independent ambient noise surface wave tomographies performed for each area annotated with letters from A to F in Figure 9.

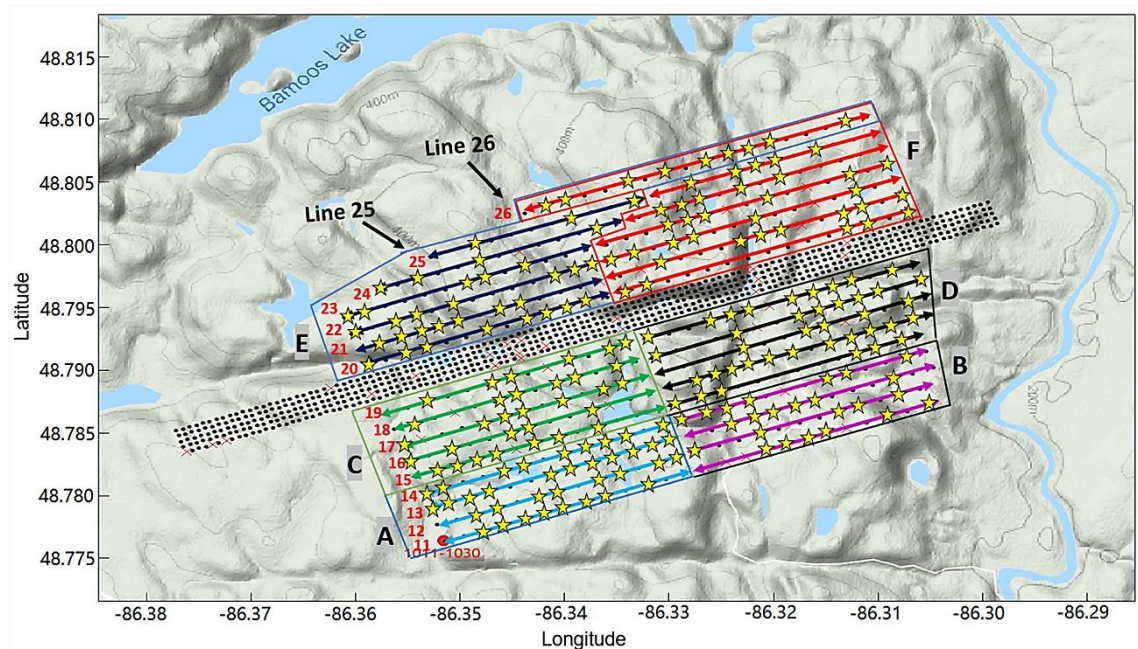


Figure 9 - Experiment design for shallow imaging using the Marathon sparse array data.

- *Figure 10* shows some dispersion curves, extracted for several virtual shot gathers belonging to lines 25 and 26. A phase velocity variation is noticed in the transition from the low-frequency band (natural noise sources) to the high-frequency band (anthropogenic noise).

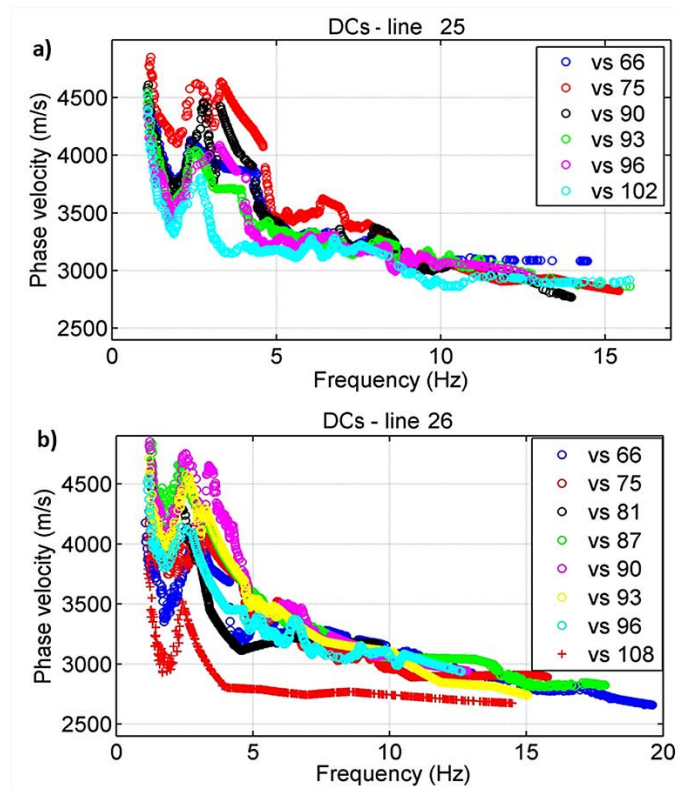


Figure 10 - Dispersion curves extracted from virtual shots belonging to line 25 (a) and line 26 (b).

Take-home messages

- The preferential azimuth and the different characteristics of the noise sources influence the phase velocity variation over the investigated area.
- Correctly merging the contribution of the natural (low frequencies) and anthropogenic (higher frequencies) noise sources, acting from preferential azimuths, allows for consistent and high-resolution imaging of the subsurface geological structure.

5. REFERENCES

- Dales, F., L. Pinzon-Rincon, F. Brenguier, P. Boué, N. Arndt, J. McBride, F. Lavoué, C. J. Bean, S. Beaupretre, R. Fayjaloun and G. Olivier (2020): Virtual sources of body waves from noise correlations in a mineral correlation context, *Seismological Research Letters*, 91 (4): 2278–2286.
- Dreiling, J. and F. Tilmann (2019): BayHunter - McMC transdimensional Bayesian inversion of receiver function and surface wave dispersion. GFZ Data Services. <https://doi.org/10.5880/GFZ.2.4.2019.001>
- Pinzon-Rincon, L., F. Lavoué, A. Mordret, P. Boué, F. Brenguier, P. Dales, Y. Ben-Zion, F. Vernon, C. J. Bean and D. Hollis (2021). Humming trains in seismology: an opportunistic source for probing the shallow crust. *Seismological Research Letters* (accepted).
- The Surface Wave Analysis Tool used for this study was developed by the research group of Politecnico di Torino (L.V. Socco, C. Comina, et al.)

Funding

PACIFIC - Passive seismic techniques for environmentally friendly and cost-efficient mineral exploration - has received funding from the European Union's Horizon 2020 research and innovation program under the grant agreement No 7766222.

<https://www.pacific-h2020.eu/>

Acknowledgements

The Marathon palladium project is under development by Generation PGM Inc. We thank John McBride for access to the exploration site and Generation's drilling database.

<https://www.genmining.com/>

We thank Nick Arndt from Sisprobe for the fruitful discussion.

<http://www.sisprobe.com/>

AUTHOR INFORMATION

<https://www.linkedin.com/in/daniela-teodor/>

ABSTRACT

Ambient noise surface wave tomography is an environmentally friendly and cost-effective seismic technique for subsurface imaging. However, noise sources acting from preferential azimuths may introduce bias in the Green's function reconstruction and in the resultant velocity models. This study, focused at the deposit scale, investigates how to correctly merge the different phase velocity measurements at various frequencies, in order to fill the gap between natural and anthropogenic noise sources.

The target is the Marathon PGE-Cu deposit (Ontario, Canada), an alkaline intrusion containing gabbros and syenites ($\phi = 25$ km). Mineralisation is hosted by gabbros close to the inward-dipping footwall of the intrusion. The country rocks are Archaean volcanic breccias. 1024 vertical-component receivers were deployed for 30 days in two overlapping grids: a 200 m x 6040 m dense array with node spacing of 50 m, and a 4000 m x 2500 m sparse array with node spacing of 150 m.

Beamforming analysis of the recorded data indicates variations in the distribution of noise. Below 5 Hz, the Lake Superior (SSW) is the dominant source of noise, while above 12 Hz, noise from the Canadian Pacific Railway and Trans-Canada highway (SW) is prominent. In the 5 - 12 Hz frequency band, surface-wave energy is dominant, and it comes from the Lake Superior and vehicle traffic. Between 12 Hz and 20 Hz, the signal is characterized by body-wave energy combined with less energetic surface waves, while above 20 Hz the imprint of body waves is dominant.

We retrieved the fundamental mode of Rayleigh wave propagation from the recorded data set. The signal was down-sampled to 50 Hz, divided into segments of 30 minutes, cross-correlated and stacked. Surface wave dispersion curves were extracted from 2-km, 1-km and 0.5 km-long arrays. Besides, various phase velocity measurements were applied. Phase-velocities were inverted to S-wave velocity structures using different probabilistic approaches.

The overall results show a high-velocity shallow anomaly, probably related to the gabbro intrusion hosting the mineralization, as well as other structures consistent with the geological model inferred from surface mapping and drill logs.